ISSN 2075-1087, Gyroscopy and Navigation, 2024, Vol. 15, No.2, pp. 21-27.
Russian Text © The Author(s), 2024, published in Giroskopiya i Navigatsiya, 2024, No.2, pp. 35-45.

Dissipation of Oscillation Energy of Hemispherical Resonator in Attachment Area

B.S. Lunin[a], M.A. Basarab[b*], R.A. Zakharyan[c]

[a]*Moscow State University, Russia*
[b]*Bauman Moscow State Technical University, Russia*
[c]*Research Institute for Civil Defense and Emergencies, Moscow, Russia*

***e-mail: bmic@mail.ru*
Received March 26, 2024; reviewed June 5, 2024; accepted June 27, 2024

Abstract: Mass defect (unbalance) of a hemispherical resonator creates forces and moments affecting its center of mass and making the resonator stem oscillate. A part of oscillation energy is dissipated in vicinity of the resonator attachment, which reduces its Q-factor and leads to additional systematic drift. The paper considers the main factors determining the dissipative characteristics of the resonator-base joint such as the resonator design and dimensions, internal friction in the bonding layer, and the defects of this layer. It has been shown that the internal friction due to attachment is proportional to the layer thickness and inversely proportional to the thickness of base, stem diameter, and Young's modulus of the layer material. Asymmetric stem fixation in the hole in base, ovality of hole or of the stem, bubbles in the bonding layer result in azimuth-depending losses and additional HRG systematic drift.

Keywords: hemispherical resonator, dissipation, hemispherical resonator gyroscope.

1. INTRODUCTION

Hemispherical resonator gyroscopes (HRGs) form a large class of modern navigation devices. They are applied to different technological areas; however, their wide distribution is limited by technical and economic reasons. One of them is the need to manufacture a quartz hemispherical resonator with high axial symmetry and Q-factor. Different geometrical deviations cause the resonator mass defect, which may largely degrade its performance and parameters of the whole HRG. Generally, geometrical shape deviations for the resonator with a mean radius R are arbitrarily distributed over the hemisphere surface. For the shell selected cross-section, its wall thickness can be described with Fourier series:

$$h(\varphi) = h_0 + \sum_{k=1}^{\infty} h_k \cos k(\varphi - \varphi_k) \qquad (1)$$

Inhomogeneous thickness of the resonator wall leads to mass distribution per unit angle, nonuniform in azimuth angle φ, following the same law:

$$m(\varphi) = m_0 + \sum_{k=1}^{\infty} m_k \cos k(\varphi - \varphi_k) \qquad (2)$$

where $m_k = \rho R^2 h_k$, ρ is the density of resonator material.

As reported in the number of publications [1–5], resonator mass defect creates forces and moments affecting its center of mass, which are directly proportional to the first, second, and third forms of this defect. For the hemispherical resonator operating on the lower bending oscillation mode, the first and third forms of the mass defect, proportional to m_1, m_3, cause the forces transverse to the symmetry axes, and the second form proportional to m_2 causes the longitudinal force. Nonuniform mass distribution over the resonator height leads to force moments, which cause the resonator stem to oscillate, the major part of oscillation energy being dissipated in the adhesive (or soldered) bonding layer, which connects the resonator stem with the base. If the energy dissipation in this joint is nonuniform and is conditioned by the vector of mass center oscillations, the resonator Q-factor depends on the orientation of the wave pattern, which provides systematic drift of the wave pattern at a rate [6]

$$\frac{d\theta}{dt} = \frac{\pi f \sin 4(\theta - \varphi_0)}{4}\left(\tilde{\xi}_1 - \tilde{\xi}_2\right) = \frac{\pi f \sin(\theta - \varphi_0)}{4}\left(\frac{1}{Q_1} - \frac{1}{Q_2}\right) \qquad (3)$$

where θ is the current attitude (orientation of antinodes) of the wave pattern; $\tilde{\xi}_1$ and $\tilde{\xi}_2$ are the maximum and minimum internal frictions in the attached resonator; Q_1 and Q_2 are the minimum and maximum Q-factors of the attached resonator; φ_0 is the attitude angle of the shell dissipative defect; f is the resonator oscillation frequency.

Amplitude of the drift rate of the wave pattern may reach several tens or even hundreds degrees per hour, and its stability depends on the constancy of internal friction (which is generally low) in the resonator-base joint. Any instability of dissipative processes in this joint results in unstable amplitude of the drift rate (3), which is understood as a random error by the navigation system. Actually it is the resonator mass unbalance and dissipation of oscillation energy near the resonator attachment that mainly cause HRG error.

This paper focuses on the major factors affecting the dissipative characteristics of the resonator-base joint such as the resonator design and dimensions, internal friction in the bonding layer, and the defects of this layer.

2. RESONATOR DESIGN AND DISSIPATION IN BONDING LAYER

In mass produced HRGs described in literature, the hemispherical resonator is usually attached to the base with an adhesive or solder alloy. Different low outgassing adhesives are commonly applied [7], and for soldering, indium, with its good adhesion to fused quartz and low melting temperature (152°C). In 1990s, Delco Electronics applied glass frit for assembly, but later abandoned this technology due to its complexity and low reliability. Some methods for adhesive-free attaching the resonator with one stem [8] or two stems [9] to the base have been proposed. The resonator is fixed with the elastic components reducing the dissipation of oscillation energy in the base. This attachment does reduce the dissipation of oscillation energy in the support; however, it degrades the dissipative stability of the joint. The elastic component mechanically contacts the quartz surface only at certain areas (contact areas). Under shocks, vibrations, temperature causing nonuniform expansion of the components and sliding, the contact conditions and the surface internal friction in the contact area vary, and so do the parameters of the systematic drift of the standing wave. Therefore, resonator mechanical attachment methods have not found practical application in HRG technology despite their obvious advantages (no outgassing, dismountability). Further we mostly consider adhesive and solder bonding layers.

Analyze how the design of hemispherical resonator affects the energy dissipation in the bonding layer. Different resonator designs have been described in publications, which can be generally classified into resonators with double-ended stems (used by Delco/Litton in 1970–2000) and with single-ended inner stems applied in the majority of modern HRGs (produced, for example, by Sagem). The attachment of HRG base with the hemispherical resonator with a single-ended inner stem is shown in Fig. 1*a*. For simplicity, only the defect of the first form of magnitude m_1 at some distance from the edge corresponding to the polar angle α is demonstrated.

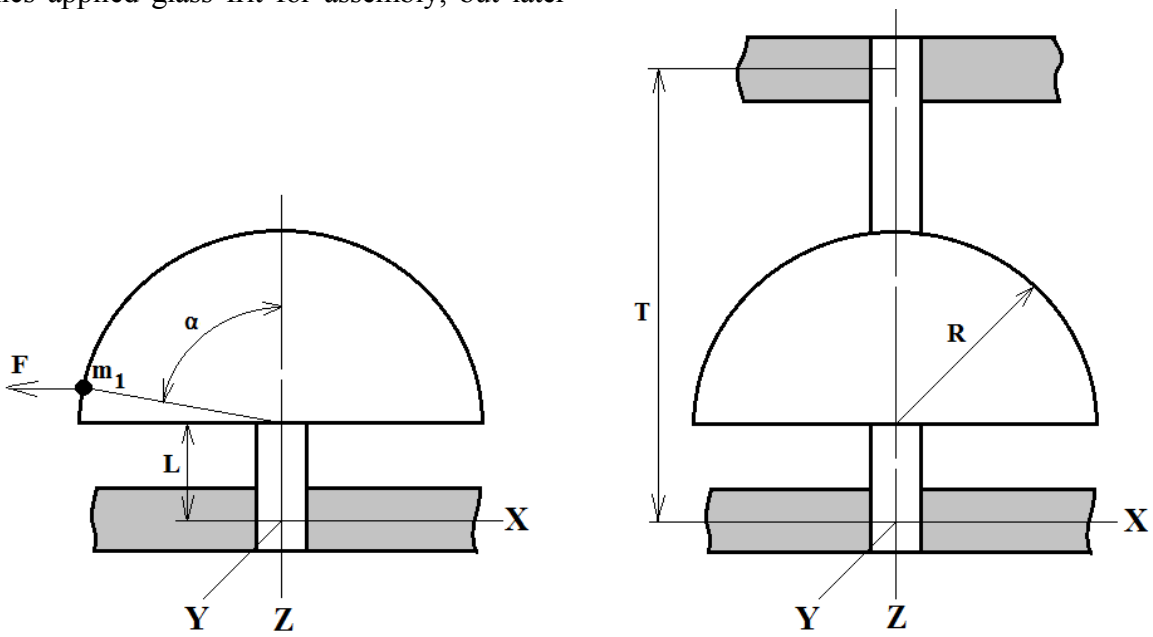

Fig. 1. Attaching the unbalanced hemispherical resonator: *a*) with inner stem; *b*) with double-ended stem

Due to the resonator shell oscillations, this mass defect creates the transverse force F, the force moment due to the resonator attachment away from its center of mass, approximately being $M_{11} = F \cdot L$, and the force moment due to the vertical motion of the shell edge $M_{12} = F \cdot R$. When applied to the bonding layer, these forces and moments cause its deformation and dissipation of the oscillation energy, thus reducing the resonator Q-factor.

Under the transverse force F, the resonator motion with respect to the base along axis X, i.e., perpendicular to the stem, can be described with the equation

$$\ddot{x} + \xi\omega\dot{x} + \frac{SE}{d_c M}x = \frac{F}{M}\cos\omega t \qquad (4)$$

where M is the resonator mass; F is the transverse force due to the mass defects; ξ is the internal friction in the bonding layer; d_c is the thickness of the bonding layer; S is the deformed area of the bonding layer; E is the Young's modulus of the layer material; ω is the oscillation circular frequency.

In the steady-state mode, the stem oscillation amplitude is

$$x_0 = \frac{F}{M\sqrt{\left(\frac{SE}{d_c M} - \omega^2\right)^2 + \xi^2\omega^4}}. \qquad (5)$$

Since most commonly $\xi^2\omega^4 << \left(\frac{SE}{d_c M} - \omega^2\right)^2$, then $x_0 \approx \frac{Fd_c}{SE}$.

The energy of the bonding layer deformation is

$$W_c = \frac{F^2 d_c}{2SE}. \qquad (6)$$

A part of this energy ΔW, irreversibly dissipated in the bonding layer, is defined as the product of the adhesive or solder internal friction ξ by the layer deformation energy:

$$\Delta W = 2\pi\xi W_c. \qquad (7)$$

The additional internal friction in the oscillator is

$$\tilde{\xi} = \frac{\xi W_c}{W},$$

where W is the resonator oscillation energy.

According to the Rayleigh formula [6],

$$W = \frac{1.52961\pi R^2 h_0 \rho a^2 \omega^2}{8}, \qquad (8)$$

where a is the amplitude of resonator oscillations.

Assuming $\alpha = \pi/2$ and $F \cong m_1 a\omega^2$ for the first form of mass defect, we obtain

$$\tilde{\xi} = \frac{4\xi d_c m_1^2 \omega^2}{1.52961 SE\pi R^2 h_0 \rho}. \qquad (9)$$

This additional internal friction forms a part of the total internal friction in the resonator. Obviously, if the resonator is balanced, i.e., $m_1 = 0$, then $\tilde{\xi} = 0$. In an unbalanced resonator, $\tilde{\xi} = \text{const}$ if the force deforming the bonding layer is independent on the orientation of the wave pattern (for example, with only first or third mass defect forms). Then the internal friction along the resonator dissipative axes increases by the same value $\tilde{\xi}$. The resonator Q-factor is degraded, however, the difference $\left(\tilde{\xi}_1 - \tilde{\xi}_2\right)$ being a cofactor in (3), remains unchanged, i.e., the systematic drift rate of the standing wave does not change. With the second form or the combination of the first and third mass defect forms, the force F becomes dependent on the orientation of the wave pattern, then $\tilde{\xi}$ becomes the function of the circular angle φ, which changes the difference $\left(\tilde{\xi}_1 - \tilde{\xi}_2\right)$ and thus the systematic drift rate.

Several useful conclusions can be made from (9). First, the additional internal friction due to attachment quadratically depends on the mass defect, so reducing the mass defects of the first three forms effectively improves the HRG accuracy. This can be achieved by enhancing the resonator manufacturing accuracy and its further balancing.

According to (9), additional losses in the resonator are proportional to the thickness of the bonding layer, so it should be minimal, and its material (adhesive or solder) should have high Young's modulus. These losses are inversely proportional to the area S, so they can be reduced by increasing the stem diameter and thickness of the base.

Note that the above relations are formally true for adhesive-free mechanical joints as well. The area of the contact areas should be used as S, and d_c and E stand for the thickness of the deformed surface layer and its Young's modulus. These parameters can be only approximately estimated, so these calculations practically do not make sense for mechanical joints.

The resonator dimensions also affect the sensitivity to the mass defects. Economically, producing smaller resonators (with smaller diameters) is more profitable,

because it downsizes the HRG and makes it more competitive. The first HRGs had ca. 60 mm resonators, and now the serially produced HRGs have 20-30 mm resonators, and they are being further reduced. Next, we discuss the problems appearing with reducing the diameter of the resonator with mass defect.

Substituting (2) to (9) demonstrates that $\tilde{\xi}$ does not depend on the resonator radius R. However, changing the resonator geometry changes its oscillation frequency according to the Rayleigh's formula [6]:

$$f = \frac{2,62h_0}{2\pi R^2}\sqrt{\frac{E_m}{3\rho(1+\upsilon)}}, \qquad (10)$$

where E_m is the Young's modulus; υ is the Poisson's ratio of the resonator material.

In order to keep the resonance frequency at units of kilohertz, the developers should decrease the resonator wall thickness while decreasing its diameter. According to the analysis of the known HRG designs [10], the wall thickness commonly makes about 6-7% of its radius. Assuming $h_0 = 0.065R$ and substituting (2) and (10) to (9), we obtain $\tilde{\xi} \sim 1/R^3$. It is well known that hemispherical resonators of mass produced HRGs are manufactured from fused quartz on special machine tools with limited accuracy [11]. If the same facilities are used, the amplitudes of harmonics of resonator geometrical deviations from the axisymmetrical shape h_k will be nearly the same independent from the resonator diameter. Then, the influence of the mass defect on systematic drift rate will grow fast as the resonator diameter decreases.

The profile of the resonator wall also matters. The resonator can be considered an absolutely rigid body if its natural frequencies exceed the frequency of the operating mode. The resonator natural frequency range depends not only on the shell diameter and thickness, but also on the stem diameter, radius of the shell-stem joint, and distance between the centers of the inner and outer hemispheres. If the frequency of shell oscillations about the stem is lower than the working frequency, the pendular oscillations of the shell are propagated to the support via the intermediate oscillator, and under certain conditions the force transmitted to the support is greatly reduced. Thus, if the frequency of shell oscillations is $N > \sqrt{2}$ times and more higher than natural frequency of the intermediate oscillator, the oscillation force transmitted to the support is reduced by N^2 times [12]. In other words, the intermediate oscillator functions as a vibration isolation between the mass-unbalanced hemispherical shell and the device base. This approach is applied, for example, in a Sagem resonator with a variable wall profile [13].

The force moments are also applied to the resonator-base joint and compensated by the moment $F_kH/2$ (Fig. 2), determined by the mass defect parameters, base thickness, and distance L. The compensating moment can be significantly reduced by reducing the moment M_{11} by moving the resonator attachment point closer to its center of mass (then $L \to 0$). The moment M_{12} can provide a significant influence, because usually $H < R$ and, with small base thickness, $F_k > F$.

Next, we consider the dissipation processes in the joints when attaching a double-stem resonator (Fig. 1*b*).

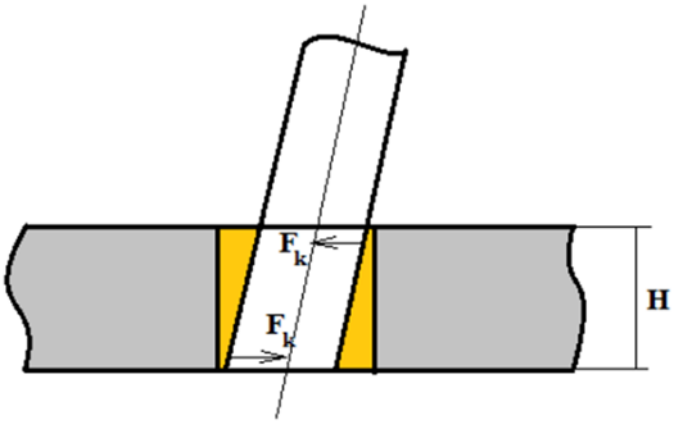

Fig. 2. Compensating the force moments at the resonator attachment point.

When attaching this resonator, the deforming force is approximately uniformly distributed between two supports. Then, with account with the quadratic dependence (6), the total energy of bonding layer deformation due to mass defects is reduced about two times, and the total energy losses in the joint will reduce, accordingly. Note that with this attachment there are no force moments in the supports, since they are compensated by relatively small transverse forces in the two supports. Thus, we can ignore the force moments due to mass defects which are present on the shell at different angles α, and balancing the resonator is reduced to removing the unbalanced mass only from its edge. The resonator balancing procedure is significantly simplified, and, despite the technological complexity of producing resonators with a double-ended stem, this design provides higher accuracy. The fact is that the residual mass unbalance of this resonator leads to a relatively small dissipation of oscillation energy in the supports, and hence to a lower Q-factor difference and amplitude of systematic drift rate of the wave pattern as compared to a resonator with one inner stem.

3. INFLUENCE OF THE BONDING LAYER INHOMOGENEITY ON DISSIPATION

Asymmetric attachment. Assume that the base hole with diameter D and the resonator stem are perfectly round, but the stem is attached asymmetrically, i.e., the bonding layer has different thickness on the opposite sides of the stem: $(d_c + \delta)$ on one side, and $(d_c - \delta)$ on the opposite side. When a variable force F is applied to the resonator stem, the bonding layer on both sides will be deformed by the same value Δh, but the deformation will be different: the layer will be compressed on one side and expand on the other side. Then the unequal elastic forces appear on the opposite sides of the stem due to different thickness of the bonding layer.

Then,

$$F = \frac{\Delta hSE}{d_c + \delta} + \frac{\Delta hSE}{d_c - \delta}. \qquad (11)$$

The deformation energies of the bonding layer on the opposite sides of the stem will be different, respectively.

The deformation energy of the bonding layer is

$$W_c = \frac{\Delta h^2}{d_c} SE\left(1 - \frac{\delta^2}{d_c^2}\right)^{-1}. \qquad (12)$$

The last cofactor in (12) considers the bonding asymmetry. For example, with asymmetry $\delta/d_c = 10\%$ the loss inhomogeneity of about 1% occurs in the attachment, which changes the systematic drift rate (3).

Ovality of the hole in the base. Assume that the resonator stem is perfectly round, symmetrically glued into the base, but the hole is oval, which changes the gap from d_c (in the direction of axis X, for example) to $(d_c + \delta)$ in the direction of axis Y. With the same force F created by the mass unbalance of the resonator, the deformation energies of the bonding layer (and, respectively, the loss of oscillation energy along these directions) will be different. Wherein

$$\frac{\Delta W_y}{\Delta W_x} = \frac{d_c + \delta}{d_c}. \qquad (13)$$

For example, if the Y axis gap is 10% larger than the X axis gap, then the energy dissipation in the Y direction is 10% more than the loss in the X direction. This difference in losses also results in additional systematic drift. The example above shows that the ovality of the hole has a much greater effect on the HRG systematic drift than the asymmetrical resonator attachment.

Air bubbles in the bonding layer. When attaching the resonator to the base, air bubbles may appear in the bonding layer, which is especially typical for adhesive joints. The bubbles also affect the energy dissipation in the joint, because the layer material deformation area S locally changes. Let us consider the ideal case, where the stem and the hole in the base are perfectly round, the stem is located symmetrically in the hole, but there is an air bubble of s area in the bonding layer. According to (6), as the area S decreases, the deformation energy of the bonding layer increases. Using formula (6), it can be shown that the deformation energy will increase $S/(S–s)$ times, also affecting the systematic drift rate.

4. INTERNAL FRICTION IN THE BONDING LAYER

Formulas (4, 5, 9) include the internal friction ξ, which characterizes the part of the deformation energy of the bonding layer that irreversibly transforms into heat. Internal friction is determined by the structure of the material, the presence of impurities, various defects, etc. The existing theories of internal friction in adhesives and metals help generally understand the reasons for their inelasticity, but the theoretical calculation of ξ is difficult even for materials with a simple composition and a known structure. Therefore, the losses in the bonding layer should be calculated using the experimental data. Internal friction in metals and alloys has been studied for several decades, so the data required for the calculations can be taken from the literature [14]. As to the internal friction in adhesives, there is very little information, and, given the wide range of modern adhesive systems, it has to be obtained experimentally.

The mechanical properties of adhesives over a rather wide temperature range are determined with dynamic thermo-mechanical analysis (DTMA): an adhesive sample is made as a thin plate, mounted on supports, and a dynamic load is applied to it using a special probe. The sample performs bending oscillations with a given frequency and amplitude selected so that the sample deformation is within a few μm. The sample bending deflection is measured while applying variable force to it. Due to internal friction, the reaction of the sample is delayed, that is a phase shift δ occurs between the applied force and the deformation. The phase shift, the load and deformation amplitudes are used to determine the viscoelastic properties of materials – Young's modulus and mechanical loss angle tangent,

which is close to ξ. The measurements are usually carried out in a thermal chamber in the temperature range from –50 to +250°C.

As an example, Figure 3 presents the experimental data obtained by this method using the thermomechanical analyzer TMA Q400 for two different types of adhesives. The curve of temperature dependence of internal friction in K-400 adhesive (Fig. 3, *a*) clearly shows a wide peak of internal friction with a maximum of ξ ≈0.38 at ~30°C, with the area of intensive internal friction covering the temperature range from –40 to +100°C. This temperature range is the most important from a practical standpoint, but in this range the internal friction in joints filled with K-400 adhesive leads to the largest energy loss in the resonator, which most significantly affects the HRG performance.

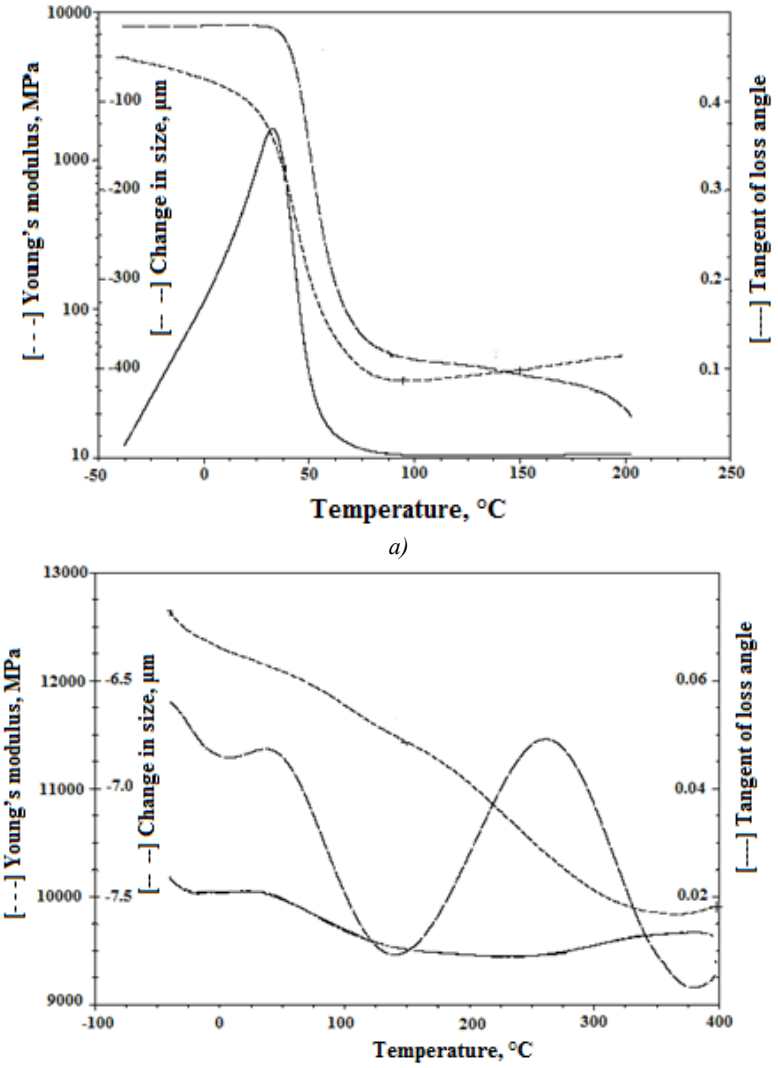

Fig. 3. Viscoelastic properties of adhesives K-400 (*a*) and Resbond-940LE (*b*) determined by DTMA.

It should also be noted that the Young's modulus of the cured adhesive changes greatly in this temperature range: it decreases from ~5000 MPa at –50°C to ~40 MPa at +150°C, which indicates significant changes in the adhesive structure. All these factors makes K-400 unsuitable for HRG assembly.

A completely different pattern is presented in Fig. 3, *b*, which shows the results of thermomechanical analysis of Resbond 940LE ceramic adhesive. The internal friction of this adhesive is 0.015-0.020, that is an order of magnitude less than in K-400, and the dependence does not have sharp extremums. The Young's modulus of the adhesive also decreases with increasing temperature, however, this decrease in the –50 to +150°C range does not exceed 10%, which manifests its much stronger and more stable structure.

Based on the known experimental dependence of internal friction in adhesive ξ(*T*), using the above formulas, the internal friction caused by attaching an unbalanced resonator with a mass defect for a given temperature can be determined.

CONCLUSIONS

The mass unbalance in the resonator leads to vibration of the resonator stem and dissipation of energy in the resonator-base bonding layer. The losses conditioned by the bonding layer are proportional to its thickness. For this reason, the layer should be made as thin as possible, for example, by using unfilled adhesive or adhesive with small (several μm) filler particles. Energy losses can also be reduced by thickening the base and/or increasing the resonator stem diameter.

When manufacturing resonators of different diameters using the same equipment, the shape error is approximately equal. In this case, the intensity of internal friction at the attachment point of unbalanced resonators is $\sim R^{-3}$.

Attaching the hemispherical resonator by two stems significantly reduces the related dissipation, which finally improves the HRG performance. Force moments created by mass defects during oscillations are compensated by relatively small transverse forces in the supports. This attachment allows removing the unbalanced mass only from the edge of the resonator during balancing and simplifies its balancing procedure.

Asymmetrical fixation of the stem in the base hole, ovality of this hole or the stem, and the presence of air bubbles in the bonding layer result in an azimuthal dependence of losses and create additional systematic drift of the HRG.

Internal friction in the bonding layer material is a composite function of temperature, so the systematic drift conditioned by these losses will also be temperature dependent.

FUNDING

This work was supported by ongoing institutional funding. No additional grants to carry out or direct this particular research were obtained.

CONFLICT OF INTEREST

The authors of this work declare that they have no conflicts of interest.

REFERENCES

1. Zhbanov, Yu.K. and Kalenova, N.V., Surface unbalance of hemispherical resonator gyroscope, Izvestiya RAN. Mekhanika tverdogo tela, 2001, no. 3, pp. 11–18.
2. Zhbanov, Yu.K. and Zhuravlev, V.F., On the balancing of hemispherical resonator gyroscope, Izvestiya RAN. Mekhanika tverdogo tela, 1998, no. 4, pp. 4–16.
3. Basarab, M.A., Matveev, V.A., Lunin, B.S., and Fetisov, S.V., Influence of nonuniform thickness of hemispherical resonator gyro shell on its unbalance parameters, Gyroscopy and Navigation, 2017, vol. 7, no. 2, pp. 97–103. https://doi.org/10.1134/S207510871702002X
4. Sharma, G.N., T. Sundararajan, and Gautam, S.S., Effect of geometric imperfections on anchor loss and characterisation of a gyroscope resonator with high quality factor, Gyroscopy and Navigation, 2020, vol. 11, no. 3, pp. 206–213. https://doi.org/10.1134/S2075108720030074
5. Gerrard, D.D., Ng, E.J., Ahn, C.H., Hong, V.A., and Kenny, T.W., Modeling the effect of anchor geometry on the quality factor of bulk mode resonators, 18th International Conference on Solid-State Sensors, Actuators and Microsystems (TRANSDUCERS), Anchorage, AK, USA, 2015, pp. 1997–2000. https://doi.org/10.1109/TRANSDUCERS.2015.7181346
6. Zhuravlev, V.F. and Klimov D.M., Volnovoi tverdotel'nyi giroskop (Wave Solid-State Gyro), Moscow: Nauka, 1985.
7. Lunin, B.S., Kreisberg, V.A., Zakharyan, R.A., and Basarab, M.A., Modelling of the residual atmosphere in vacuum device with internal adhesive joints, Vacuum, 2021, vol. 184, 109964. https://doi.org/10.1016/j.vacuum.2020.109964
8. Sapozhnikov, A.I., Vinogradov, I.E., Dotsenko, E.S., Vvedenskii, M.D., Timofeev, S.S., Kolesnik, M.M., Izmailov, E.A., and Molchanov, A.V., Hemispherical resonator gyroscope, RF patent RU 2793299, 2023.
9. Izmailov, E.A., Kolesnik, M.M., Usyshkin, O.G., Kan, S.G., and Izmailov, A.E., Hemispherical resonator gyroscope, RF patent RU 2164006, 2001.
10. Maslov, A.A., Maslov, D.A., Ninalalov, I.G., and Merkuryev, I.V., Hemispherical resonator gyros (An overview of publications), Gyroscopy and Navigation, 2023, vol. 14, no. 1, pp. 1–13. https://doi.org/10.1134/S2075108723010054
11. Ma, Z., Zhao, H., Zhao, W., Song, X., and Chen, X., Precisions forming technology of quartz hemispherical harmonic oscillator, Navigation and Control, 2019, vol. 18, no. 2, pp. 77–95. https://doi.org/10.3969/j.issn.1674-5558.2019.02.012
12. Timoshenko, S.P., Kolebaniya v inzhenernom dele (Oscillations in Engineering), Moscow: Nauka, 1967.
13. James, M. and Jeanroy, A., Resonator particularly for a vibrating gyroscope, US Patent application 2006/0169068.
14. Postnikov, V.S., Vnutrennee trenie v metallakh (Internal Friction in Metals), Moscow: Metallurgiya, 1968.